Distributed Robust Sliding-Mode Control For Multiple Parallel Interlinking Converters Under Unknown Disturbances

Chang Yang, *Student Member, IEEE*, Tao Zheng, Pengyu Li, Ming Bu and Josep M. Guerrero, *Fellow, IEEE*

***Abstract*—Parallel interlinking converters (ICs) find application in high-power hybrid AC/DC microgrids. However, challenges exist in achieving coordinated control among different ICs for power sharing, which is beyond this parallel structure and encompasses the interplay between different subgrids. The existing approach suffers from a heavy communication burden and sensitivity to disturbances. To address this issue, this paper proposes a distributed robust sliding-mode control (SMC) for the hybrid AC/DC microgrid with parallel ICs, ensuring the convergence of multiple control objectives within a predetermined time slot. An observer is designed to mitigate disturbances for a reduction in the required controller gain and suppression of chattering issues. The stability of the proposed control strategy is analyzed using the Lyapunov theory and control parameters are designed based on the stability analysis. Experiments under various working conditions demonstrate the outperformance of the proposed method compared to traditional distributed control approaches.**

***Index Terms*—distributed control, hybrid AC/DC microgrid, parallel interlinking converters, sliding mode control, disturbance compensation**

NOMENCLATURE

$i, \mathcal{N}_{\text{ic}}$	Index and number of parallel ICs.
G	Undirected graph composed of parallel ICs.
A, D	Adjacent matrix and degree matrix of the graph G.
$\mathbb{V}, \mathbb{E}, \mathbb{N}$	Set of vertices, edges and neighbor vertices.
$P^{\text{ref}}, Q^{\text{ref}}$	Active and reactive power reference.
$u^{\text{pc}}, u^{\text{sc}}$	Input of primary control and secondary control.
ω_c	Cut-off frequency of power filter.
$U_{\text{od}}, U_{\text{oq}}$	AC voltage in d-axis and q-axis.
$I_{\text{od}}, I_{\text{oq}}$	Current flowing through the filter inductance in d-axis and q-axis.
P, P^{set}	Output value and setting value of active power.
m, n	Droop slopes of dual-droop control.
$f^{\text{pu}}, U_{\text{dc}}^{\text{pu}}$	Normalized value of AC frequency and DC voltage.
$f^{\text{max}}, f^{\text{min}}$	Setting value of maximum AC frequency and minimum AC frequency.
$U_{\text{dc}}^{\text{max}}, U_{\text{dc}}^{\text{min}}$	Setting value of maximum DC voltage and minimum DC voltage.
ξ, M	Unknown disturbances and its upper bound.
t_{pre}	Predetermined time for convergence
$P^{\text{pu}}, P^{\text{rated}}$	Unit value and rated value of active power.
l	Flag to indicate the leader IC.
S	Switching function of sliding mode control
$e^{\text{P}}, e^{\text{fv}}$	Power error and balance error
$u^{\text{sw}}, u^{\text{eq}}$	Input of switching control and equivalent control.
$u^{\text{law}}, u^{\text{es}}$	Input of control law and disturbance observer.
P^{es}	Estimated value of active power.
$\text{sign}(\cdot)$	Symbolic function
α, β	Parameters of control law.
τ, σ	Parameters of disturbance observer.

This work is supported by the National Natural Science Foundation of China (No.U23B20112) and Natural Science Foundation of Shaanxi Province (No.2024JC-YBMS-420). *(Corresponding author: Tao Zheng).*

Chang Yang, Tao Zheng, and Ming Bu are with the Shaanxi Key Laboratory of Smart Grid, School of Electrical Engineering, Xi'an Jiaotong University, 710049 Xi'an, China (e-mail: yangchang1996@stu.xjtu.edu.cn, tzheng@mail.xjtu.edu.cn, bm1234@stu.xjtu.edu.cn)

Pengyu Li is with the Yunnan Electric Power Dispatching and Control Center, China Southern Power Grid, 650011 Kunming, China.

Josep M. Guerrero is with the Department of Energy Technology, Aalborg University, DK-9220 Aalborg, Denmark, and also with the Department of Electric Engineering, Technical University of Catalonia, Barcelona 08019, Spain (email: joz@energy.aau.dk, josep.m.guerrero@upc.edu) .

I. INTRODUCTION

Microgrid (MG) is one of the promising approaches for integrating distributed generation (DG), as it enhances both the efficiency and reliability of electrical power consumption [1]. Numerous researches have focused on developing coordinated control strategies to achieve power sharing [2]–[5], unbalance compensation [6]–[8] and power quality improvements [9]–[11] in single AC microgrid (ac-MG) or DC microgrid (dc-MG). However, the coordinated control strategy for hybrid MGs requires further improvement, primarily due to the unclear relationship between the electrical quantities in the two subgrids. The interlinking converter (IC) serves as a bridge to transfer active power between ac-MG and dc-MG. It involves the frequency of the ac-MG, the voltage of the dc-MG and the power delivered through the IC.

Although a single IC offers ease of control, parallel ICs are more suitable for high-power applications. This parallel configuration ensures mutual redundancy among different devices, and a failure in one IC does not lead to the disconnection of the AC and DC subgrids. However, potential challenges,

such as power circulation among different ICs, cannot be overlooked as they reduce the overall efficiency of the hybrid MG. Distributed coordinated control based on a hierarchical structure is an effective way to address this issue [12]. In this control framework, multiple controllers collaborate with each other by exchanging information with their neighbors, making it particularly suitable for hybrid AC/DC MGs to facilitate the cooperation among different types of DGs [13] and MGs [14]. For instance, in [15] and [16], distributed control strategies are applied to achieve active power sharing and economic power dispatch in hybrid MGs with parallel ICs. However, the coordination among different ICs requires the communication network linking ICs and DGs, which complicates the entire system. In [17]–[19], distributed proportional-integral (PI) controllers are developed for power management and current sharing. Nevertheless, these controllers are designed based on a linear control paradigm, making them prone to disturbances and changes in working conditions [20].

Compared to linear control structures, the application of nonlinear control to MGs represents a novel research focus. Various types of nonlinear control have been developed, such as model predictive control (MPC) [21], [22], model-free control [23], [24] and sliding mode control (SMC) [25]–[27]. Among these advanced control strategies, MPC employs the system model to predict state variables and track reference trajectories, which can be applied in the field of hybrid MG. In [21], a detailed mathematical model of ICs is established to regulate output voltage and power. In [22], an economic power output model of the MG is presented to minimize the overall cost. MPC provides good control performance and disturbance rejection capabilities; however, it requires complex system modeling processes. Consequently, several model-free control strategies [23], [24] have been explored to address this issue, although their disturbance rejection capabilities have yet to be fully verified. Sliding mode control (SMC), another form of nonlinear control, can achieve disturbance rejection by employing high controller gains, which is comparable to MPC. It has been applied to MG control, especially in hybrid MGs. In [25] and [26], distributed SMC strategies are proposed to deal with actuator faults and system parameter uncertainties respectively. In [27], distributed direct power control is developed based on SMC in an ac-MG. These approaches demonstrate good performance in terms of control accuracy, even in the presence of external disturbances. However, there is a trade-off between the controller gain and the anti-disturbance capability. Higher controller gain enhances the system's ability to counteract disturbances but introduces significant chattering in the steady-state operation.

To improve the control performance of hybrid AC/DC MGs under unknown disturbances, this paper proposes a distributed robust SMC with disturbance observers. This method ensures effective coordination among multiple parallel ICs by employing advanced control strategies. The main contributions are summarized as follows.

1) A SMC-based distributed control strategy is proposed to coordinate the parallel ICs, which simultaneously achieves the control objectives of both power sharing among different ICs and balance control between ac-MG and dc-MG. The proposed control strategy mitigates power circulation among the ICs, thereby enhancing the power efficiency of hybrid MGs.
2) A designed observer is integrated into the proposed control strategy to compensate for the unknown disturbances, which allows for the prediction of various disturbance types. This observer facilitates a substantial reduction in the design of the SMC controller gain.
3) The stability of the proposed control strategy is demonstrated by using the Lyapunov theory. Control parameters are estimated to ensure the attainment of multiple control objectives within a predetermined time slot.

The rest of this paper is organized as follows. The system architecture of the hybrid AC/DC MG with parallel ICs is presented in Section II and the distributed robust SMC strategy with disturbance observer is proposed in Section III. In Section IV, experiments are carried out to validate the performance of the proposed control strategy under various operating conditions. Finally, conclusions are given in Section V.

II. Hybrid AC/DC MG with Multiple Parallel Interlinking Converters

A. System Architecture

Fig.1 illustrates the topology of a hybrid AC/DC MG with multiple parallel ICs. In this hybrid structure, different droop control strategies are applied, such as P-f and Q-U_{ac} droop in ac-DG and P_{dc}-U_{dc} droop in dc-DG. Multiple ICs are paralleled to achieve high power rating, which keeps the power balance between AC subgrid and DC subgrid. Without loss of generality, a single droop-controlled ac-DG is used to represent the interconnected ac-DGs integrated into the AC bus and the dc-MGs can be modeled similarly.

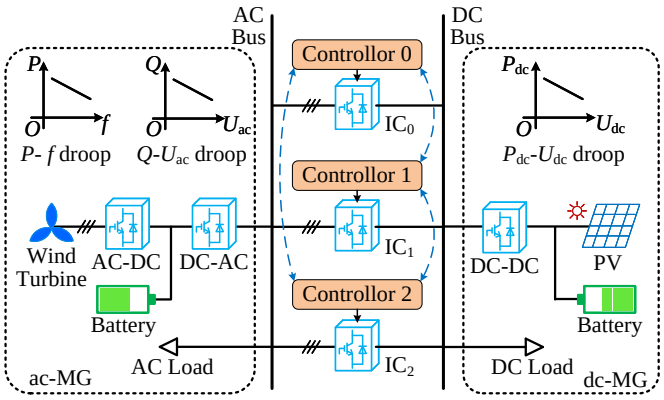

Fig. 1. A hybrid AC/DC MG with parallel ICs and their distributed communication network

B. Communication Network

As shown in Fig.1, a distributed communication network is illustrated with blue dashed lines, which can be represented as an undirected graph $G = (\mathbb{V}, \mathbb{E}, A)$ with $\mathcal{N}_{\text{ic}}$ vertices. If the edge $(i, j) \in \mathbb{E}$, the element of adjacency matrix $a_{ij} = a_{ji} = 1$. The degree matrix of the undirected graph G can be expressed as $D = \text{diag}_i(d_i)$, where $d_i = \sum_{j \in \mathbb{N}_i} a_{ij}$.

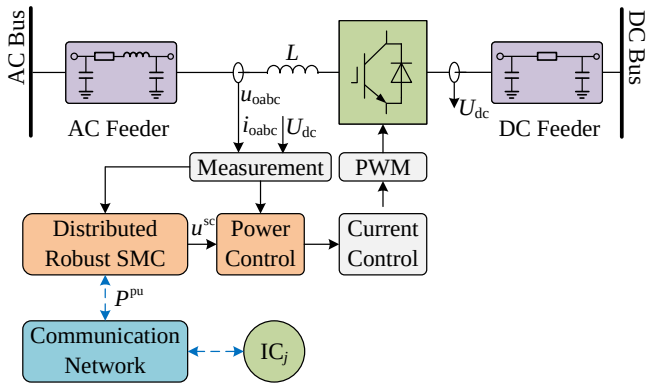

Fig. 2. Overview of distributed control among parallel ICs

III. Distributed Robust Sliding-Mode Control with Disturbance Observer

A. Overview

Fig.2 presents an overview of distributed control among parallel ICs. Different ICs exchange power information through the communication network. The distributed robust SMC uses the information from the neighbor ICs to generate the power command u_i^{sc}, which serves as the secondary control. By combining the primary control command u_i^{pc} with u_i^{sc}, the power control provides a reference, as expressed in Eq.(1). It should be noted that this paper focuses on the active power sharing of parallel ICs, and reactive power support to the ac-MG is not considered.

$$\begin{cases} P_i^{\text{ref}} = u_i^{\text{pc}} + u_i^{\text{sc}} \\ Q_i^{\text{ref}} = 0 \end{cases} \tag{1}$$

In the power control, a first-order low-pass filter is usually used to smooth the active power, which can be denoted by Eq.(2).

$$\dot{P}_i = -\omega_c P_i + 1.5\omega_c(U_{\text{od}i} I_{\text{od}i} + U_{\text{oq}i} I_{\text{oq}i}) \tag{2}$$

Regarding the primary control, the normalized values of AC frequency and DC voltage are employed to implement the dual-droop control [23], which can be expressed by Eq.(3).

$$u_i^{\text{pc}} = P_i^{\text{set}} - m_i f_i^{\text{pu}} + n_i U_{\text{dc}i}^{\text{pu}} \tag{3}$$

where f_i^{pu} and $U_{\text{dc}i}^{\text{pu}}$ are the normalized valued, defined as follows.

$$f_i^{\text{pu}} = \frac{f_i - 0.5(f^{\max} + f^{\min})}{0.5(f^{\max} - f^{\min})}$$

$$U_{\text{dc}i}^{\text{pu}} = \frac{U_{\text{dc}i} - 0.5(U_{\text{dc}}^{\max} + U_{\text{dc}}^{\min})}{0.5(U_{\text{dc}}^{\max} - U_{\text{dc}}^{\min})}$$

According to Eq.(1)–Eq.(3), the active power delivered by IC$_i$ can be denoted as Eq.(4) considering the presence of unknown disturbance.

$$\begin{cases} \dot{P}_i = f(P_i) + \omega_c(u_i^{\text{sc}} + \xi_i) \\ f(P_i) = \omega_c(P_i^{\text{set}} - P_i) - \omega_c(m_i f_i^{\text{pu}} - n_i U_{\text{dc}i}^{\text{pu}}) \end{cases} \tag{4}$$

Generally, the disturbance ξ_i originates from measurement errors, communication issues, or cyber attacks [25], [28]. Herein, it is assumed that ξ_i is bounded by an upper limit M, i.e. $|\xi_i| < M$

B. Control Objectives

This subsection outlines the control objectives for the coordinated control of parallel ICs. The primary goals include power sharing among different ICs, balance control between ac-MG and dc-MG, and disturbance compensation to mitigate external influences. These objectives are crucial for improving the efficiency of hybrid MGs with parallel ICs. Herein, each objective will be mathematically formulated and discussed in detail.

1) Power Sharing: Due to the different line impedances connected to the subgrids, power circulation among the ICs is inevitable. To address this issue, it is essential to distribute the active power transmitted by each IC according to their rated capacities. This approach helps to avoid overload and reduce power circulation. The control objective of power sharing can be mathematically expressed by Eq.(5).

$$P_i^{\text{pu}}(t) = P_j^{\text{pu}}(t),\ i,j \in \mathbb{V},\ \forall t \in [t_{\text{pre}}, \infty) \tag{5}$$

where $P_i^{\text{pu}} = P_i / P_i^{\text{rated}}$ represents the per-unit value of IC$_i$'s output power.

2) Balance Control: To maintain the power balance between ac-MG and dc-MG, the objective of balance control is expressed by Eq.(6). A leader of the parallel ICs is selected to balance the f_i^{pu} and $U_{\text{dc}i}^{\text{pu}}$. With this objective, a relationship between the AC frequency of the ac-MG and the DC voltage of the dc-MG can be established. The uniformity of the electrical quantity deviation ensures the power balance between different subgrids.

$$l_i(m_i f_i^{\text{pu}}(t) - n_i U_{\text{dc}i}^{\text{pu}}(t)) = 0,\ i \in \mathbb{V},\ \forall t \in [t_{\text{pre}}, \infty) \tag{6}$$

where $l_i = 1$ if IC$_i$ is selected as the leader IC, otherwise, $l_i = 0$

3) Disturbance Compensation: To compensate for disturbances in the secondary control, an observer is employed to estimate the disturbances ξ_i. Consequently, a predictive term u_i^{es} is introduced within the observer to ensure that Eq.(7) is satisfied.

$$\lim_{t\to\infty} |u_i^{\text{es}} - \xi_i| = 0\ \forall i \in \mathbb{V} \tag{7}$$

C. Distributed Robust Sliding-Mode Controller Design

According to the fundamental principles of SMC denoted by Eq.(8), the design of a sliding-mode controller generally comprises two key components: the sliding surface $S_i = 0$ and the control law u_i^{sc}. In the proposed control strategy, a disturbance observer is also introduced to achieve the objective specified in Eq.(7). The subsequent sections will elaborate on the design methodology of this distributed robust sliding-mode controller.

$$u_i^{\text{sc}} = \begin{cases} u_i^{\text{sc+}},\ S_i > 0 \\ u_i^{\text{sc-}},\ S_i < 0 \end{cases} \tag{8}$$

1) Sliding Surface: Firstly, considering the control objectives of power sharing and balance control outlined in Section III-B, the error of control objectives e_i can be defined as Eq.(9).

$$e_i = e_i^{\mathrm{P}} + l_i e_i^{\mathrm{fv}} \tag{9}$$

where e_i^{P} and e_i^{fv} corresponds to the objectives Eq.(5) and Eq.(6) respectively, which can be expressed by Eq.(10) and Eq.(11).

$$e_i^{\mathrm{P}} = \frac{P_i^{\mathrm{rate}}}{d_i} \sum_{j \in \mathbb{N}_i} a_{ij} (P_i^{\mathrm{pu}} - P_j^{\mathrm{pu}}) \tag{10}$$

$$e_i^{\mathrm{fv}} = m_i f_i^{\mathrm{pu}} - n_i U_{\mathrm{dc}i}^{\mathrm{pu}} \tag{11}$$

The error consists of two parts: power error e_i^{P} and balance error e_i^{fv}. The power error utilizes the power information from the neighbor ICs. If $e_i^{\mathrm{P}} = 0$, the power sharing between IC_i and its neighbor ICs can be achieved, subsequently leading to the realization of global power sharing. The balance error has two functions: first, it aims to evenly distribute the load between the two subgrids, and second, it compensates for the deviation introduced by the dual-droop control.

The design of the sliding surface is based on the error e_i [29]. Herein, a straightforward sliding surface is selected as Eq.(12). With this design, reaching the sliding surface ($S_i = 0$) and achieving control objectives ($e_i = 0$) are equivalent, which facilitates control implementation and stability analysis. In this paper, the chattering issue of SMC caused by this simple sliding surface will be addressed through the design of disturbance observer.

$$S_i = e_i = 0 \tag{12}$$

2) Control Law: The control law comprises switching control and equivalent control, which can be expressed in Eq.(13). The switching control follows a symbolic function, ensuring the system remains on the sliding surface by altering the control direction whenever the surface is crossed. Herein, the switching control can be designed as shown in Eq.(14).

$$u_i^{\mathrm{law}} = u_i^{\mathrm{sw}} + u_i^{\mathrm{eq}} \tag{13}$$

$$u_i^{\mathrm{sw}} = -\frac{1}{\omega_c}(\alpha \mathrm{sign}(S_i) + \beta S_i) \tag{14}$$

where $\alpha, \beta > 0$ are two parameters, which determine the dynamic process of SMC.

The equivalent control utilizes the equivalent model of the IC described in Eq.(4) to keep it on the sliding surface, which can be designed to ensure $\dot{P} = 0$ when the disturbance $\xi_i = 0$.

$$u_i^{\mathrm{eq}} = -\frac{1}{\omega_c} f(P_i) \tag{15}$$

3) Disturbance Observer: In the traditional SMC approaches [26], [27], disturbance rejection is typically achieved by increasing the controller gain α. This generally necessitates that α should be larger than the upper bound of the disturbance M. However, this method has several limitations: Firstly, a higher controller gain cannot completely eliminate the effects of disturbances (as discussed in Section IV-E). Additionally, an excessively high gain may induce chattering in the SMC [27]. Therefore, a disturbance observer is introduced as an alternative approach to enhance disturbance rejection performance without the drawbacks associated with high controller gains.

According to the equivalent model in Eq.(4), the observer can be designed as Eq.(16) to achieve the control objectives outlined in Eq.(7).

$$\begin{cases} \dot{P}_i^{\mathrm{es}} = f(P_i) + \omega_c u_i^{\mathrm{law}} + \tau(P_i - P_i^{\mathrm{es}}) \\ \dot{u}_i^{\mathrm{es}} = \sigma(P_i - P_i^{\mathrm{es}}) \end{cases} \tag{16}$$

4) Controller Implementation: According to Eq.(13)–Eq.(16), the proposed coordinated control strategy for multiple parallel ICs can be expressed by Eq.(17), which includes the switching control u_i^{sw}, the equivalent control u_i^{eq} and the disturbance observer u_i^{es}. The detailed control diagram of the proposed distributed robust SMC is illustrated in Fig.3. It is important to note that Eq.(17) is the implement of the general concept described in Eq.(8). The difference between $u_i^{\mathrm{sc+}}$ and $u_i^{\mathrm{sc-}}$ depends on the switching control input u_i^{sw}, which varies based on the sign of S_i.

$$u_i^{\mathrm{sc}} = u_i^{\mathrm{sw}} + u_i^{\mathrm{eq}} - u_i^{\mathrm{es}} \tag{17}$$

D. Stability Analysis and Parameter Design

In this subsection, the stability of the proposed robust control strategy is verified using the Lyapunov theory. The Lyapunov function, defined as shown in Eq.(18), serves as the basis for this analysis.

$$\begin{aligned} V_i &= V_{i1} + V_{i2} \\ &= \frac{\omega_c}{2\sigma}(u_i^{\mathrm{es}} - \xi_i)^2 + \frac{1}{2}(P_i^{\mathrm{es}} - P_i)^2 + \frac{1}{2}S_i^2 \end{aligned} \tag{18}$$

where $V_{i1} = \frac{\omega_c}{2\sigma}(u_i^{\mathrm{es}} - \xi_i)^2 + \frac{1}{2}(P_i^{\mathrm{es}} - P_i)^2$, which is differentiated in Eq.(19).

$$\dot{V}_{i1} = \frac{\omega_c}{\sigma}(u_i^{\mathrm{es}} - \xi_i)(\dot{u}_i^{\mathrm{es}} - \dot{\xi}_i) + (P_i^{\mathrm{es}} - P_i)(\dot{P}_i^{\mathrm{es}} - \dot{P}_i) \tag{19}$$

By substituting Eq.(4) and Eq.(16) into Eq.(19), Eq.(20) can be obtained.

$$\dot{V}_{i1} = -\tau(P_i^{\mathrm{es}} - P_i)^2 - \frac{\dot{\xi}_i}{\sigma}\omega_c(u_i^{\mathrm{es}} - \xi_i) \tag{20}$$

where the parameters τ and σ can be designed to ensure $\dot{V}_{i1} < 0$, thus the inequality Eq.(21) can be obtained.

$$\tau > -\frac{\dot{\xi}_i}{\sigma} \times \frac{\omega_c(u_i^{\mathrm{es}} - \xi_i)}{(P_i^{\mathrm{es}} - P_i)^2} \tag{21}$$

It is important to note that $\dot{\xi}_i/\sigma = 0$ can be guaranteed by selecting a large value of σ to make $\dot{V}_{i1} = -\tau(P_i^{\mathrm{es}} - P_i)^2$. According to the Lasalle's invariance theorem, $\lim_{t\to\infty}(P_i^{\mathrm{es}} - P_i) = 0$ is reasonable and the control objective $\lim_{t\to\infty}|u_i^{\mathrm{es}} - \xi_i| = 0$ can be achieved.

The second term of the Lyapunov function, $V_{i2} = \frac{1}{2}S_i^2$, can be differentiated as shown in Eq.(22).

$$\begin{aligned} \dot{V}_{i2} = S_i\dot{S}_i &\le -(\alpha|S_i| + \beta|S_i|^2 - \omega_c(\xi_i - u_i^{\mathrm{es}})S_i) \\ &\le -\beta|S_i|^2 - (\alpha - \omega_c(\xi_i - u_i^{\mathrm{es}}))|S_i| \end{aligned} \tag{22}$$

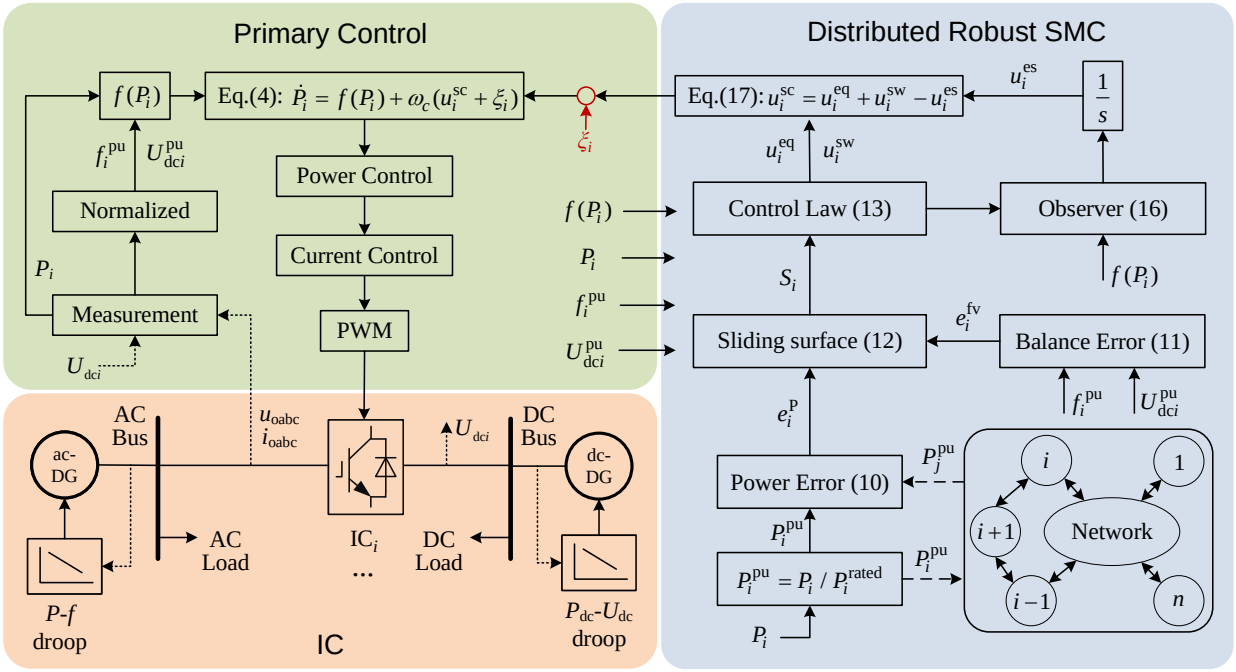

Fig. 3. Control diagram of distributed robust SMC for IC_i

Therefore, the parameter α should be designed as Eq.(23) to ensure $\dot{V}_{i2} \leq -\beta|S_i|^2 < 0$.

$$\alpha > \omega_c|\xi_i - u_i^{\mathrm{es}}| \tag{23}$$

The compensator u_i^{es} allows for the selection of a small value of α because $u_i^{\mathrm{es}} \approx \xi_i$. Without compensation, α should be greater than $\omega_c M$, which is the primary cause of chattering.

According to the parameter design in Eq.(21) and Eq.(23), the inequality Eq.(24) associated with the Lyapunov function holds and the proposed SMC-based control strategy is asymptotic stable.

$$\dot{V}_i = \dot{V}_{i1} + \dot{V}_{i2} < -\beta|S_i|^2 < 0 \tag{24}$$

Furthermore, the proposed control strategy can reach the control objectives within a predetermined time t_{pre}. The parameter β can be selected to ensure convergence within a finite time. According to Eq.(22), the inequality Eq.(25) holds, and Eq.(26) can be obtained by integrating both sides of the inequality.

$$S_i\dot{S}_i < -\beta|S_i|^2 \tag{25}$$

$$\int_{S_i(0)}^{S_i(t_{\mathrm{pre}})} \frac{1}{S_i} dS_i < -\int_0^{t_{\mathrm{pre}}} \beta dt \tag{26}$$

Considering $S_i(t_{\mathrm{pre}}) = 0$, the parameter β can be designed by Eq.(27).

$$\beta < (e^{S_i(0)} - 1)/t_{\mathrm{pre}} \tag{27}$$

where $S_i(0)$ is the initial value of the switching function.

IV. Experimental Results

A. Experiment Setup

To verify the control performance of the proposed control strategy under the unknown disturbances, several experiments are conducted in a hybrid AC/DC MG with multiple parallel ICs. The experimental platform is shown in Fig.4a, and its topology is depicted in Fig.4b. In the experiment, a voltage source converter (VSC) and a programmable DC power supply serve as the ac-DG and dc-DG respectively, with droop controls implemented. At the start of the experiment, a $900+300j$ VA AC load and a 600 W DC load are connected to their respective buses. Three VSCs are connected in parallel to function as multiple ICs, with IC0 designated as the leader. The parameters of the experimental platform are detailed in TABLE I. Two different controllers are used to implement different control strategies. The primary control of the IC is executed by the TMS320F28335 DSP controller configured in the VSC, which is responsible for the sampling and PWM generation. Both the sampling and switching frequency are set to 10 kHz, and the DSP controller performs one control calculation step after each sampling. The proposed robust control strategy is deployed on Raspberry Pi controllers using the Python programming language. Each IC is equipped with a Raspberry Pi controller. All parameters used for the control strategy implementation are listed in TABLE II. The DSP controller and Raspberry Pi controller are connected through a high-speed CAN serial bus to upload output power information and issue power instructions. Different Raspberry Pi controllers communicate with each other through a router using the UDP protocol, with a communication frequency of 100 Hz.

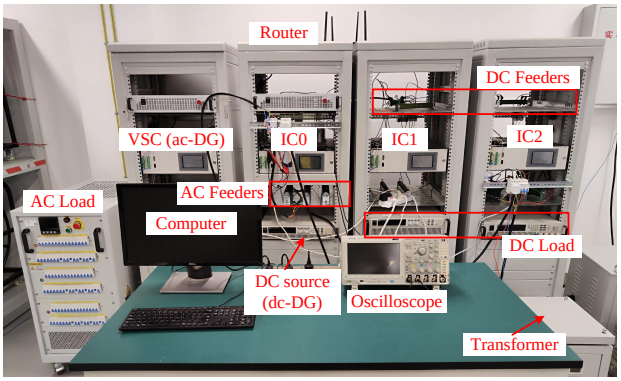

(a)

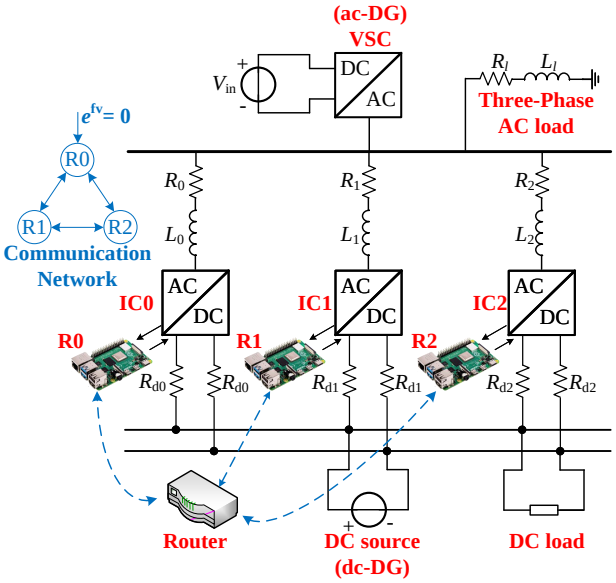

(b)

Fig. 4. Experiment platform of the hybrid MG with parallel ICs. (a) instruments, (b) grid overview

In the experiment, the disturbances injected into the system are generated through an algorithm implemented in the DSP controller, which can produce various types of disturbances. Herein, several common disturbance signals are considered, including constant disturbance, sinusoidal disturbance, and slope disturbance. The specific locations of the disturbance injections are indicated in Fig.3 and Eq.(4), where ξ_i represents the disturbance injected into IC_i.

B. Control Performance

In this experiment, the control performance of the proposed control strategy is verified under two different working conditions: one without disturbances and the other with different types of disturbances.

1) Without Disturbances: Herein, the experiment is manipulated in four stages: i. At $t = 20s$, the proposed control strategy is put into operation, ii. At $t = 40s$, decrease 300W active load in the dc-MG, iii. At $t = 60s$, increase 900W active load in the dc-MG, iv. At $t = 80s$, increase 300W active load in the ac-MG. The experiment results are shown in Fig.5. The control objective of power sharing is set as

TABLE I
SYSTEM PARAMETERS OF THE HYBRID MG IN THE EXPERIMENT

Classification	Parameters	value
IC	AC RMS voltage	173V
	Frequency	50Hz
	DC voltage	300V
	Filter inductance	1.2mH
	Filter capacitor	16uF
	Switching frequency	10kHz
Feeders	R_0, L_0	0.4Ω, 0.33mH
	R_1, L_1	1.1Ω, 2.67mH
	R_2, L_2	0.7Ω, 1.45mH
	R_{d0}	0.5Ω
	R_{d1}	1Ω
	R_{d2}	2Ω

TABLE II
CONTROL PARAMETERS IN THE EXPERIMENT

Parameter	Value	Parameter	Value
$f^{\min}$	49.5Hz	$f^{\max}$	50.5Hz
$U_{\mathrm{dc}}^{\min}$	280V	$U_{\mathrm{dc}}^{\max}$	320V
m_i	0.5kW	n_i	0.5kW
α	10	β	1
τ	10	σ	200
ω_c	$2\pi\times20$rad/s	$\vec{l}$	{1,0,0}

$P_{\mathrm{IC0}} : P_{\mathrm{IC1}} : P_{\mathrm{IC2}} = 1 : 1 : 1$, while IC0 acts as the leader to ensure $e_0^{\mathrm{fv}} = 0$. According to the results, power sharing among different ICs can be achieved after the implementation of the proposed control strategy. The balance error is minimized and eventually approaches 0. Furthermore, the control performance remains stable under step load changes.

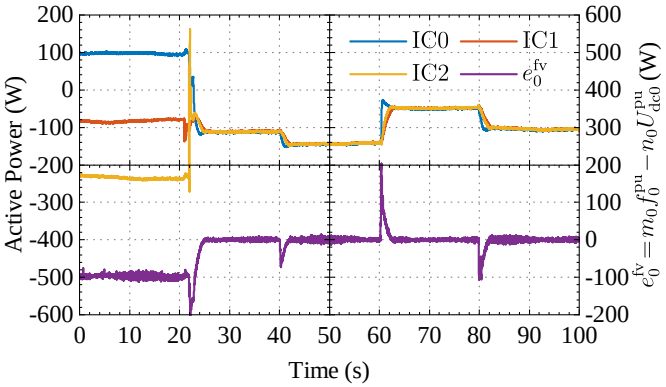

Fig. 5. Experiment results for control performance verification under the working condition without disturbances.

2) With Disturbances: Under an uncertain working condition, secondary control is prone to disturbance and its performance declines. This experiment focuses on assessing the dynamic process of the proposed control strategy under different types of disturbances. It assumes that the power command of the secondary control is subjected to constant,

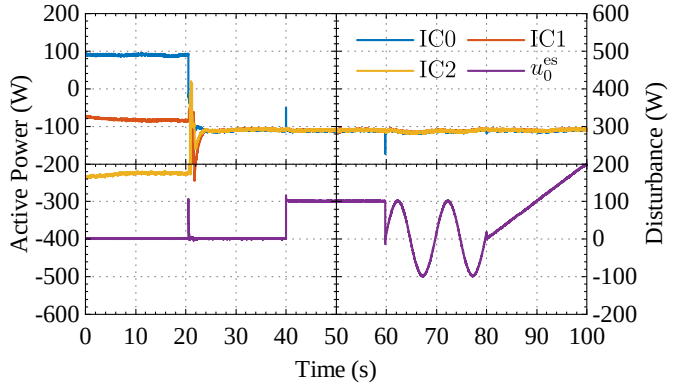

(a)

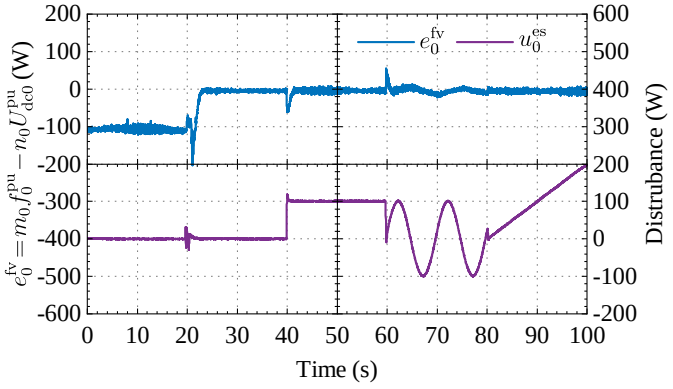

(b)

Fig. 6. Experiment results under different types of disturbances. (a) output power of ICs, (b) balance error

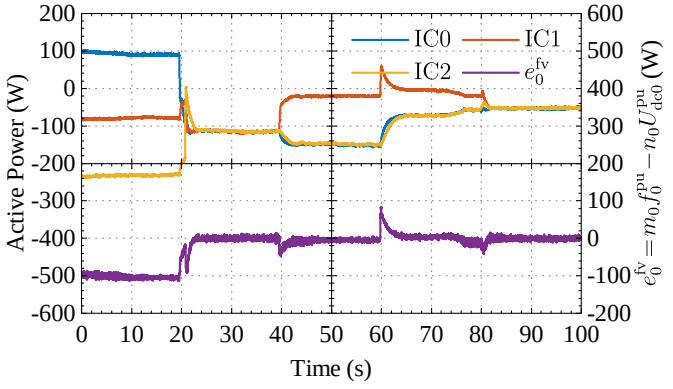

Fig. 7. Experiment results under IC1 communication failure at $t = 40s$.

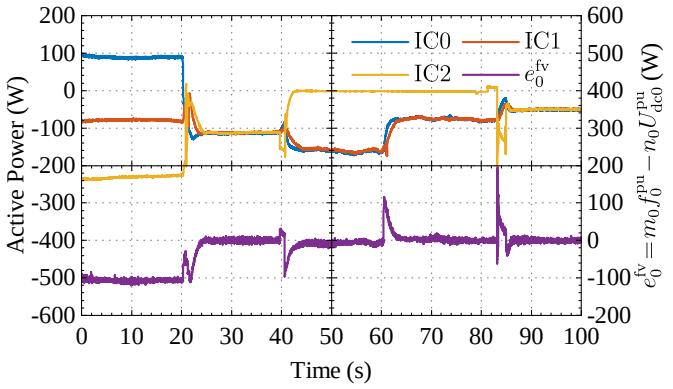

Fig. 8. Experiment results under IC2 plug and play

sinusoidal, and slope disturbances. This experiment consists of four stages: i. the proposed control strategy is put into operation at $t = 20s$, ii. a constant disturbance $\xi_0 = 100$W is introduced to impact IC0 at $t = 40s$, iii. the sinusoidal disturbance of $\xi_0 = 100\sin(2\pi \times 0.1t)$ W is applied at $t = 60s$, iv. the slope disturbance of $\xi_0 = 10t$ W appears at $t = 80s$. The experiment results are illustrated in Fig.6, where the output power of ICs and the balance error are shown in Fig.6a and Fig.6b respectively. It is apparent that the disturbance can be accurately predicted using the observer, i.e. $u_0^{es} = \xi_0$. Good control performance is maintained under multiple disturbances, as it can be effectively preserved through compensation.

C. Communication Failure

In the proposed control strategy, the control system can maintain stable when some of the communication links fail. Herein, an experiment is conducted to simulate an IC1 communication failure. At $t = 20s$, the proposed control strategy is put into operation. At $t = 40s$, the communication of IC1 fails. At $t = 60s$, a 600 W active load is added to the dc-MG, and the communication of IC1 recovers at $t = 80s$. The experiment results are shown in Fig.7. After the communication failure, the deviation in the output power of IC1 is observed, but there is no adverse impact on the stability of the system. Once the communication recovers, global power sharing among all ICs can be achieved immediately.

D. Plug and Play

In this experiment, the control performance is evaluated through the plug-and-play functionality of IC2. The stages of the experiment are as follows: IC2 switches off at $t = 40s$ and restarts at $t = 80s$. When IC2 is out of service, the active load of dc-MG increases 600W at $t = 60s$. The results are shown in Fig.8. When IC2 quits, power sharing among the remaining ICs is successfully achieved. Upon its restart, the re-accessed IC can negotiate with the existing ICs, and the output of all ICs comes to an agreement.

E. Comparison

In this subsection, experiments are conducted for control performance comparison in the presence of unknown disturbances. To do so, a linear PI controller [14] and traditional SMC [27] are utilized. In the experiments, coordinated control among parallel ICs is activated at $t = 25s$ and a sinusoidal disturbance $\xi_0 = 100\sin(2\pi \times 0.1t)$W is introduced into the control system at $t = 50s$. Two different controller gains ($\alpha = 10$ and $\alpha = 20000$) are applied in the traditional SMC to evaluate control performance, where $\alpha = 10$ matches the gain used in the proposed control strategy. According to the results presented in Fig.9, neither the linear PI controller

TABLE III
COMPARISON WITH STATE-OF-THE-ART CONTROL STRATEGIES FOR INTERLINKING CONVERTER

	Multiple parallel	Controller type	Implementation	Disturbance rejection
[17]	√	linear	simple	×
[18]	√	linear	simple	×
[19]	√	linear	simple	×
[21]	×	MPC	complex	√
[23]	×	model-free	middle	×
[30]	×	ANN	complex	√
Proposed	√	SMC	middle	√

nor the traditional SMC can achieve the control objectives mentioned in Section III-B under the disturbance ξ_0. This is particularly evident when the traditional SMC has a low gain ($\alpha = 10$), its control performance may be inferior to that of the linear PI controller. Therefore, the traditional SMC requires a large α to mitigate the disturbance. Despite this, the disturbance still affects its control performance. In contrast, the proposed control strategy performs better due to the design of the disturbance observer, which fully compensates for the output power fluctuations caused by the disturbance.

Furthermore, the proposed method is compared with state-of-the-art control strategies for the IC, including traditional linear controllers in [17]–[19], MPC in [21], model-free control in [23] and artificial neural network (ANN)-based controller in [30]. The comparative results are summarized in TABLE III. Firstly, most studies about the coordination of multiple parallel ICs rely on traditional linear controllers. Although these controllers are structurally simple and easy to implement, their robustness, particularly in disturbance rejection, needs further improvement. Advanced control strategies primarily focus on single IC, with limited research addressing multiple parallel scenarios. Among these, MPC and ANN demonstrate effective disturbance rejection through complex control strategy design, whereas the disturbance rejection capability of model-free control requires further validation. The proposed control strategy modifies the traditional SMC to balance design complexity and robustness. It is suitable for applications where linear controllers are inadequate and high robustness is required.

V. CONCLUSION

This paper presents a distributed robust SMC for multiple parallel ICs in hybrid AC/DC MGs. The proposed strategy addresses multiple control objectives simultaneously, including power sharing among all ICs and power balance between ac-MG and dc-MG. The robustness is further enhanced through integrated disturbance observer. Theoretical analysis demonstrates that the stability of the controller can be guaranteed with appropriate parameter selection, and the control objectives can be achieved within a predetermined time slot. Experiment results verify the effectiveness of the proposed control strategy, which ensures a high level of control performance under different types of disturbances. Compared to

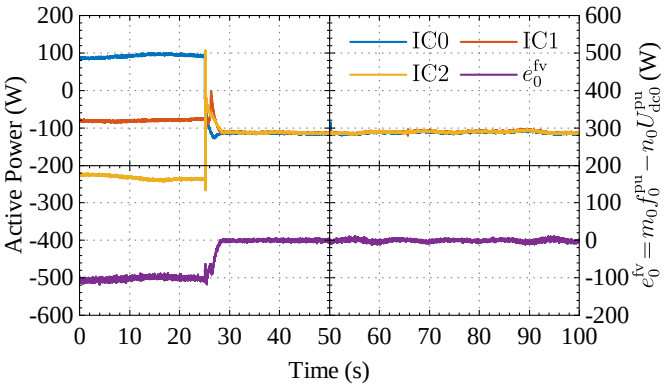

(a)

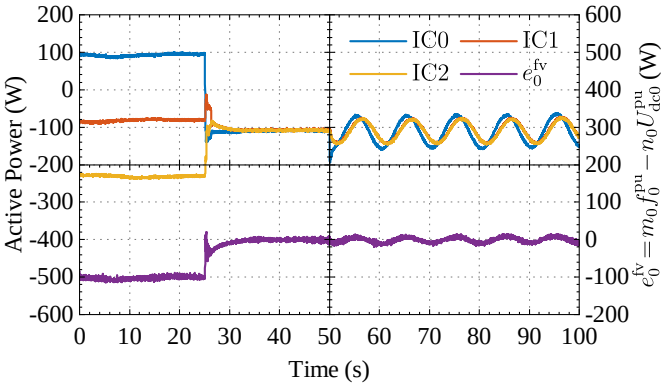

(b)

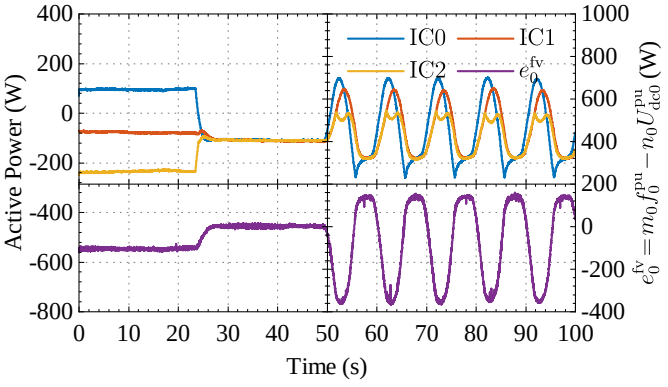

(c)

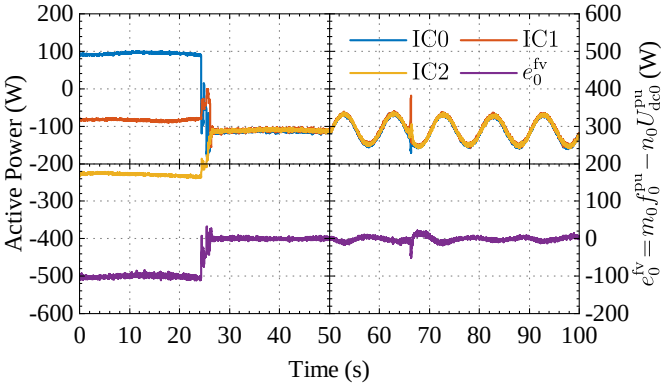

(d)

Fig. 9. Experiment results under different control strategies. (a) proposed robust SMC with the disturbance observer, (b) PI controller, (c) traditional SMC ($\alpha = 10$), (d) traditional SMC ($\alpha = 20000$).

traditional PI-based and SMC-based approaches, the proposed strategy is more effective at resisting unknown disturbances and maintaining its original control performance.

REFERENCES

[1] D. E. Olivares, A. Mehrizi-Sani, A. H. Etemadi, C. A. Cañizares, R. Iravani, M. Kazerani, A. H. Hajimiragha, O. Gomis-Bellmunt, M. Saeedifard, R. Palma-Behnke *et al.*, "Trends in microgrid control," *IEEE Trans. Smart Grid*, vol. 5, no. 4, pp. 1905–1919, 2014.

[2] J. Choi, S. I. Habibi, and A. Bidram, "Distributed finite-time event-triggered frequency and voltage control of AC microgrids," *IEEE Trans. Power Syst.*, vol. 37, no. 3, pp. 1979–1994, 2022.

[3] Y. Zeng, Q. Zhang, Y. Liu, X. Zhuang, and H. Guo, "Hierarchical cooperative control strategy for battery storage system in islanded DC microgrid," *IEEE Trans. Power Syst.*, vol. 37, no. 5, pp. 4028–4039, 2022.

[4] Q. Zhang, Y. Zeng, Y. Liu, X. Zhuang, H. Zhang, W. Hu, and H. Guo, "An improved distributed cooperative control strategy for multiple energy storages parallel in islanded DC microgrid," *IEEE Trans. Emerg. Sel. Topics Power Electron.*, vol. 10, no. 1, pp. 455–468, 2022.

[5] R. Wang, D. Ma, M.-J. Li, Q. Sun, H. Zhang, and P. Wang, "Accurate current sharing and voltage regulation in hybrid wind/solar systems: An adaptive dynamic programming approach," *IEEE Trans. Consum. Electron.*, vol. 68, no. 3, pp. 261–272, 2022.

[6] J. Lu, B. Zhang, X. Hou, and J. M. Guerrero, "A distributed control strategy for unbalanced voltage compensation in islanded AC microgrids without continuous communication," *IEEE Trans. Ind. Electron.*, vol. 70, no. 3, pp. 2628–2638, 2023.

[7] A. Navas-Fonseca, C. Burgos-Mellado, J. S. Gómez, F. Donoso, L. Tarisciotti, D. Sáez, R. Cárdenas, and M. Sumner, "Distributed predictive secondary control for imbalance sharing in AC microgrids," *IEEE Trans. Smart Grid*, vol. 13, no. 1, pp. 20–37, 2022.

[8] Y. Han, P. Shen, X. Zhao, and J. M. Guerrero, "An enhanced power sharing scheme for voltage unbalance and harmonics compensation in an islanded AC microgrid," *IEEE Trans. Energy Convers.*, vol. 31, no. 3, pp. 1037–1050, 2016.

[9] Z. Zhao, J. Zhang, B. Yan, R. Cheng, C. S. Lai, L. Huang, Q. Guan, and L. L. Lai, "Decentralized finite control set model predictive control strategy of microgrids for unbalanced and harmonic power management," *IEEE Access*, vol. 8, pp. 202 298–202 311, 2020.

[10] Z. Ma, Z. Wang, Y. Guo, Y. Yuan, and H. Chen, "Nonlinear multiple models adaptive secondary voltage control of microgrids," *IEEE Trans. Smart Grid*, vol. 12, no. 1, pp. 227–238, 2021.

[11] Y. Li, Z. Zhang, T. Dragičević, and J. Rodriguez, "A unified distributed cooperative control of DC microgrids using consensus protocol," *IEEE Trans. Smart Grid*, vol. 12, no. 3, pp. 1880–1892, 2021.

[12] J. M. Guerrero, J. C. Vasquez, J. Matas, L. G. de Vicuna, and M. Castilla, "Hierarchical control of droop-controlled AC and DC microgrids—a general approach toward standardization," *IEEE Trans. Ind. Electron.*, vol. 58, no. 1, pp. 158–172, 2011.

[13] H.-J. Yoo, T.-T. Nguyen, and H.-M. Kim, "Consensus-based distributed coordination control of hybrid AC/DC microgrids," *IEEE Trans. Sustain. Energy*, vol. 11, no. 2, pp. 629–639, 2020.

[14] J. Zhou, H. Zhang, Q. Sun, D. Ma, and B. Huang, "Event-based distributed active power sharing control for interconnected AC and DC microgrids," *IEEE Trans. Smart Grid*, vol. 9, no. 6, pp. 6815–6828, 2018.

[15] E. Espina, R. Cárdenas-Dobson, J. W. Simpson-Porco, D. Sáez, and M. Kazerani, "A consensus-based secondary control strategy for hybrid AC/DC microgrids with experimental validation," *IEEE Trans. Power Electron.*, vol. 36, no. 5, pp. 5971–5984, 2021.

[16] Z. Li, Z. Cheng, J. Si, and S. Li, "Distributed event-triggered hierarchical control to improve economic operation of hybrid AC/DC microgrids," *IEEE Trans. Power Syst.*, vol. 37, no. 5, pp. 3653–3668, 2022.

[17] P. Lin, P. Wang, C. Jin, J. Xiao, X. Li, F. Guo, and C. Zhang, "A distributed power management strategy for multi-paralleled bidirectional interlinking converters in hybrid AC/DC microgrids," *IEEE Trans. Smart Grid*, vol. 10, no. 5, pp. 5696–5711, 2019.

[18] J. Wang, C. Dong, C. Jin, P. Lin, and P. Wang, "Distributed uniform control for parallel bidirectional interlinking converters for resilient operation of hybrid AC/DC microgrid," *IEEE Trans. Sustain. Energy*, vol. 13, no. 1, pp. 3–13, 2022.

[19] F. Nejabatkhah, Y. W. Li, and K. Sun, "Parallel three-phase interfacing converters operation under unbalanced voltage in hybrid AC/DC microgrid," *IEEE Trans. Smart Grid*, vol. 9, no. 2, pp. 1310–1322, 2018.

[20] N. M. Dehkordi, N. Sadati, and M. Hamzeh, "Distributed robust finite-time secondary voltage and frequency control of islanded microgrids," *IEEE Trans. Power Syst.*, vol. 32, no. 5, pp. 3648–3659, 2017.

[21] Y. Shan, J. Hu, K. W. Chan, Q. Fu, and J. M. Guerrero, "Model predictive control of bidirectional dc–dc converters and ac/dc interlinking converters—a new control method for pv-wind-battery microgrids," *IEEE Trans. Sustain. Energy*, vol. 10, no. 4, pp. 1823–1833, 2018.

[22] J. Hu, Y. Shan, Y. Yang, A. Parisio, Y. Li, N. Amjady, S. Islam, K. W. Cheng, J. M. Guerrero, and J. Rodríguez, "Economic model predictive control for microgrid optimization: A review," *IEEE Trans. Smart Grid*, vol. 15, no. 1, pp. 472–484, 2023.

[23] H. Zhang, J. Zhou, Q. Sun, J. M. Guerrero, and D. Ma, "Data-driven control for interlinked AC/DC microgrids via model-free adaptive control and dual-droop control," *IEEE Trans. Smart Grid*, vol. 8, no. 2, pp. 557–571, 2017.

[24] C. Yang, T. Zheng, M. Bu, P. Li, and J. M. Guerrero, "Distributed model-free adaptive control strategy for hybrid ac/dc microgrid with event-triggered mechanism," *IEEE Trans. Ind. Electron.*, vol. 71, no. 8, pp. 9077–9086, 2024.

[25] M. A. Shahab, B. Mozafari, S. Soleymani, N. M. Dehkordi, H. M. Shourkaei, and J. M. Guerrero, "Distributed consensus-based fault tolerant control of islanded microgrids," *IEEE Trans. Smart Grid*, vol. 11, no. 1, pp. 37–47, 2019.

[26] A. Pilloni, A. Pisano, and E. Usai, "Robust finite-time frequency and voltage restoration of inverter-based microgrids via sliding-mode cooperative control," *IEEE Trans. Ind. Electron.*, vol. 65, no. 1, pp. 907–917, 2017.

[27] C. Alfaro, R. Guzman, L. G. de Vicuña, H. Komurcugil, and H. Martín, "Distributed direct power sliding-mode control for islanded AC microgrids," *IEEE Trans. Ind. Electron.*, vol. 69, no. 10, pp. 9700–9710, 2021.

[28] Y. Seyedi, H. Karimi, and J. M. Guerrero, "Centralized disturbance detection in smart microgrids with noisy and intermittent synchrophasor data," *IEEE Trans. Smart Grid*, vol. 8, no. 6, pp. 2775–2783, 2017.

[29] H. R. Baghaee, M. Mirsalim, G. B. Gharehpetian, and H. A. Talebi, "A decentralized power management and sliding mode control strategy for hybrid AC/DC microgrids including renewable energy resources," *IEEE Trans. Ind. Informat.*, 2017.

[30] S. Jha, B. Singh, and S. Mishra, "Control of ilc in an autonomous ac–dc hybrid microgrid with unbalanced nonlinear ac loads," *IEEE Trans. Ind. Electron.*, vol. 70, no. 1, pp. 544–554, 2022.

Chang Yang (Student Member, IEEE) received the B.S. and M.S. degrees in electrical engineering from the School of Electrical Engineering, Xi'an Jiaotong University, Xi'an, China in 2018 and 2021, respectively, where he is currently pursuing the Ph.D. degree in electrical engineering.

His current research interests include control and protection of microgrid, renewable energy, and advanced control techniques.

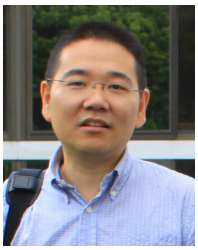

Tao Zheng received the B.S., M.S. and Ph.D. degrees in electrical engineering from the School of Electrical Engineering, Xi'an Jiaotong University, Xi'an, China in 1999, 2003, and 2007, respectively, where he is currently an Associate Professor.

His current research interests include power system communications, distribution network fault location and microgrid control.

Pengyu Li received the B.S. and M.S. degrees in electrical engineering from the School of Electrical Engineering, Xi'an Jiaotong University, Xi'an, China in 2021 and 2024, respectively. He is currently with the Yunnan Electric Power Dispatching and Control Center, China Southern Power Grid, Kunming, China.

His current research interest includes power system operation and control.

Ming Bu received the B.S. degree in electrical engineering from the School of Electrical Engineering, Xi'an Jiaotong University, Xi'an, China in 2022, where she is currently pursuing the M.S. degree in electrical engineering.

Her main research interests include coordination control of energy router.

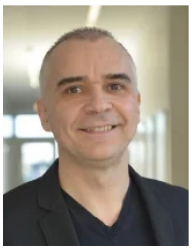

Josep M. Guerrero (Fellow, IEEE) received the B.S. degree in telecommunications engineering, the M.S. degree in electronics engineering, and the Ph.D. degree in power electronics from the Technical University of Catalonia, Barcelona, in 1997, 2000 and 2003, respectively. Since 2011, he has been a Full Professor with the Department of Energy Technology, Aalborg University, Denmark, where he is responsible for the Microgrid Research Program. From 2019, he became a Villum Investigator by the Villum Fonden, which supports the Center for Research on Microgrids (CROM) at Aalborg University, being the founder and the Director of the same center. In 2023, he joined the Technical University of Catalonia as an ICREA Research Professor.

His research interests are oriented to different microgrid aspects, including power electronics, distributed energy-storage systems, hierarchical and cooperative control, energy management systems, and optimization of microgrids and islanded minigrids.